

## Pressure of two-dimensional Yukawa liquids

This content has been downloaded from IOPscience. Please scroll down to see the full text.

2016 J. Phys. D: Appl. Phys. 49 235203

(<http://iopscience.iop.org/0022-3727/49/23/235203>)

View [the table of contents for this issue](#), or go to the [journal homepage](#) for more

Download details:

IP Address: 202.195.129.247

This content was downloaded on 06/05/2016 at 14:12

Please note that [terms and conditions apply](#).

# Pressure of two-dimensional Yukawa liquids

Yan Feng<sup>1</sup>, J Goree<sup>2</sup>, Bin Liu<sup>2</sup>, Lei Wang<sup>1</sup> and Wen-de Tian<sup>1</sup>

<sup>1</sup> Center for Soft Condensed Matter Physics and Interdisciplinary Research, College of Physics, Optoelectronics and Energy, Soochow University, Suzhou 215006, People's Republic of China

<sup>2</sup> Department of Physics and Astronomy, The University of Iowa, Iowa City, IA 52242, USA

E-mail: [fengyan@suda.edu.cn](mailto:fengyan@suda.edu.cn)

Received 26 January 2016, revised 26 March 2016

Accepted for publication 4 April 2016

Published 6 May 2016



CrossMark

## Abstract

A simple analytic expression for the pressure of a two-dimensional Yukawa liquid is found by fitting results from a molecular dynamics simulation. The results verify that the pressure can be written as the sum of a potential term which is a simple multiple of the Coulomb potential energy at a distance of the Wigner–Seitz radius, and a kinetic term which is a multiple of the one for an ideal gas. Dimensionless coefficients for each of these terms are found empirically, by fitting. The resulting analytic expression, with its empirically determined coefficients, is plotted as isochores, or curves of constant area. These results should be applicable to monolayer dusty plasmas.

Keywords: Yukawa liquids, dusty plasma, molecular dynamics simulation

(Some figures may appear in colour only in the online journal)

## 1. Introduction

Without externally applied force, pressure is an intrinsic physical quantity of a fluid. From equations of state [1] of gases, for example, the ideal gas law [2] and the van der Waals equation [3], pressure is a function of the temperature and volume, and maybe other physical quantities. The expressions of pressure for liquids are more complicated, due to much more complex equations of state [4] of liquids. As calculation power has increased, more computer simulations have been used to obtain accurate expressions of pressure for various forms of matter [5, 6].

In this paper, we use molecular dynamical (MD) simulations to study the pressure of two-dimensional (2D) Yukawa liquids. The Yukawa (or Debye–Hückel) potential, also called the screened Coulomb potential [7], has the form of a Coulomb potential with an exponential decay,  $\phi(r) = Q^2 \exp(-r/\lambda_D) / 4\pi\epsilon_0 r$ , where  $\lambda_D$  is the Debye screening length and  $Q$  is the particle charge. It has been found to describe particle interactions for example in dusty plasmas [8] and colloids [9]. The exponential decay in the interparticle interaction comes from the shielding effects of two kinds of free charges, like electrons and positive ions for dusty plasmas [10], or negative and positive ions for colloids [9].

A dusty plasma [11–15] is a four-component mixture, where three components fill the entirety of a 3D volume; these are the electrons, ions, and neutral gas. The fourth component

of charged dust particles, however, experiences very different confining forces than the electrons and ions so that dust particles occupy a much smaller volume. Gravity plays an important role in the confinement of these massive dust particles, but not for ions and electrons under laboratory conditions. Within the entire 3D laboratory volume, there are huge numbers of electrons and ions, but very few dust particles, which can sediment due to gravity so that they become isolated in a single horizontal layer (monolayer), also called a 2D dusty plasma [10, 16–23]. Because of their high particle charge<sup>3</sup>  $Q$  and low charge-to-mass ratio, these dust particles are strongly coupled, so that a collection of dust particles exhibits properties of solids or liquids. Here we will focus on the liquid state. Over the past twenty years, experimenters using monolayer dusty plasmas have studied liquid phenomena such as transport [17] and waves [19]. Experimenters also found that the interparticle potential, in a monolayer dusty plasma, is nearly a repulsive Yukawa [8] for particles located in a plane perpendicular to ion flow. This experimental result is the justification for using the Yukawa potential in 2D dusty plasma simulations

<sup>3</sup> In typical 2D dusty plasma experiments, dust particles are not too many, typically  $10^4 \sim 10^5$ , occupying only a razor-thin monolayer, as compared with enormous numbers of electrons and ions that fill the entire plasma chamber volume. Consequently, the dust particles do not affect the electrons, ions, or gas in any meaningful way. Only in multiple-layer dusty plasmas, or especially 3D dusty plasmas, do the dust particles in an experiment perturb electrons and ions, for example by electron depletion.

such as [24–27]. However, the interaction can differ from a Yukawa potential for multi-layer or three-dimensional dust clouds [28], where some particles are located in the wakes of other particles, due to the ion flow. For 2D dusty plasmas, the dust-particle-component has a pressure of its own, unrelated to the pressure of the electrons and ions, due to the weak 2D spatial occupation of dust particles as compared with the massive 3D occupation of electrons and ions. Within this 2D plane, the mutual repulsion of dust particles is the source of the potential contribution of the pressure of the monolayer dust component. Here, we are concerned with the pressure of the dust component, in such a monolayer dusty plasma.

In analogy to the experiments, where only the dust particles are observed, simulations such as [29–42] are often performed with a simplification that only the dust particle motion is tracked. In this simplification, the physics of the electrons and ions is represented as the microscopic screening length, while the physics of the gas molecules is represented by a prescribed kinetic temperature of the dust particles. For 2D Yukawa liquids, previous simulations using this simplification include [29–38], which were all for uniform conditions. These simulations assume that particles are constrained to move on a 2D plane; this assumption is justified by observations in monolayer dusty plasma experiments, such as in [10], where particles have negligible out-of-plane motion and the plane never buckles. This one-component simulation approach has been validated experimentally for phenomena such as phonon spectra [43–45] that do not involve charge separation of the electrons and ions. It is important to note, however, that this one-component approach would not be appropriate for certain non-uniform conditions, such as a dust-acoustic wave in a three-dimensional dust cloud, in which the electrons and ions move oppositely in response to a nonuniformity. The validity of the present paper, where we use a one component Yukawa model, is therefore limited to uniform conditions in a monolayer dusty plasma, but not dust acoustic waves for example.

Typically 2D Yukawa systems are characterized using two dimensionless quantities: the coupling parameter  $\Gamma$  and the screening parameter  $\kappa$ , defined [34] as

$$\Gamma = Q^2/(4\pi\epsilon_0ak_B T)$$

and

$$\kappa \equiv a/\lambda_D,$$

where  $T$  is the particle kinetic temperature and

$$a = (n\pi)^{-1/2}$$

is the Wigner–Seitz radius [35] for an areal number density  $n$ . The coupling parameter  $\Gamma$  is proportional to the inverse temperature  $1/T$ , while the screening parameter  $\kappa$  indicates the volume or number density<sup>4</sup> of Yukawa systems, related to

<sup>4</sup>In 2D dusty plasma experiments, besides the shielding factor of the Yukawa interaction, the radial confinement would also affect the compressibility of dust suspension. Typically, the three-dimensional confinement can be modeled as a combination of the radial confinement and a vertical parabolic potential well. The vertical well allows out-of plane motion of dust particles. If this vertical confinement is weak, the compressibility of the system could be affected by a buckling deformation. In our current simulation, we assume the limit of an infinitely strong vertical confinement, as in other 2D dusty plasma simulations such as [30, 35].

the density, or the volume (or the area for 2D systems) of one particle. In the one-component plasma description:  $\Gamma \sim 1$  for a nonideal gas,  $\Gamma > 1$  for a liquid, and there is a solid for  $\Gamma$  of order  $10^2$ , where the solid–liquid transition depends on  $\kappa$ , as shown by simulations [30, 36] for 2D Yukawa systems. Here we study the liquid state.

Here we use simulations to seek a relation between the pressure and temperature for various ‘volumes’ of a 2D Yukawa liquid. Our approach is to calculate the pressure using the diagonal elements of the stress tensor computed from the positions and velocities of all the individual dust particles, as explained in section 2.2. This method differs from three previous calculations of pressure for 2D Yukawa liquids based on MD simulations: Totsuji *et al* [46, 47] computed the internal energy  $U$  from a simulation, and from that obtain the pressure; Hartmann *et al* [30] computed the pressure from the pair correlation function from a simulation; Vaulina *et al* [48, 49] used a semi-empirical jumps theory.

We will propose a simple analytic expression for the pressure, as the sum of a potential term and a kinetic term that is proportional to temperature. Coefficients for this analytic approximation are obtained by fitting simulation results for various temperatures and densities. Comparing the magnitude of the potential and kinetic terms, we will find that the potential term dominates for most of the parameter space studied here. In a recent experiment [50], it has been discovered that a strongly coupled monolayer dusty plasma seems to obey the ideal-gas equation of state, which suggests that the kinetic contribution of the pressure plays an important role in some parameter regimes.

## 2. Simulation

### 2.1. Method

We perform equilibrium MD simulations [33] to study 2D Yukawa liquids dynamics. We integrate the equation of motion  $m\ddot{\mathbf{r}}_i = -\nabla\Sigma_j\phi_{ij}$  for all simulated 1024 particles, where  $\phi_{ij}$  is the binary interparticle interaction with a Yukawa potential [8]. The Yukawa potential is truncated at distances beyond a cutoff radius of  $24.8a$ , as justified in [37]. All simulated particles are constrained within a single 2D plane, in a rectangular box, with a width-to-length ratio of 0.866 and periodic boundary conditions. We do not include any Langevin heating term or frictional cooling term. From test simulations, we have confirmed that our pressure results are independent of the simulated particle number from 1024 to 16 384.

As inputs, we set the parameters of  $\kappa$  and  $\Gamma$  in our simulations. We specify eleven values of  $\kappa$  over an experimentally relevant range of 0.5–3.0, while keeping the areal number density  $n$  as constant for all runs. For each value of  $\kappa$ , as mentioned above, the 2D Yukawa lattice has one specific melting point [30, 36], which can be expressed as  $1/\Gamma_{\text{melt}}$ . In our simulation, we change the desired temperature over a wide range: from the coldest temperature at just  $\approx 1\%$  higher than this melting point, to the hottest at  $\approx 70$  times higher than this melting point. As justified in [37], the integration time step is chosen from the range between  $(0.0037\text{--}0.037)\omega_{\text{pd}}^{-1}$  depending on the

$\Gamma$  value, where  $\omega_{pd} = (Q^2/2\pi\epsilon_0ma^3)^{1/2}$  [35] is the nominal 2D dusty plasma frequency, where  $m$  is the mass of one dust particle. The values we choose for the time step are  $0.0037\omega_{pd}^{-1}$  for  $1.0 \leq \Gamma < 4.0$ ,  $0.0093\omega_{pd}^{-1}$  for  $4.0 \leq \Gamma < 10.0$ ,  $0.0185\omega_{pd}^{-1}$  for  $10.0 \leq \Gamma < 40.0$ , and  $0.037\omega_{pd}^{-1}$  for  $\Gamma \geq 40.0$ . We verified that the time step is adequately small so that energy is conserved quite well.

The temperatures  $T$  that we report are kinetic temperatures computed from the mean square velocity fluctuation. These values can differ 1% from the input target value, due to fluctuations arising from the finite system size. The input target value for temperature is specified by a Nosé–Hoover thermostat, which is only used for the initial  $10^5$  steps to reach the desired temperature. After that initialization, the thermostat is turned off and the next  $10^5$  steps are integrated under steady conditions, with no thermostat. The data reported in this paper for pressure are based on the  $10^5$  steps without the thermostat.

## 2.2. Pressure calculation

We obtain the pressure of the 2D Yukawa system from the stress tensor. Using the MD simulation data for particle positions, velocities and potentials, we calculate the diagonal elements of the stress tensor,

$$P_{xx}(t) = \sum_{i=1}^N \left[ mv_{ix}v_{ix} - \frac{1}{2} \sum_{j=i}^N \frac{x_{ij}x_{ij}}{r_{ij}} \frac{\partial \Phi(r_{ij})}{\partial r_{ij}} \right], \quad (1)$$

and similarly for  $P_{yy}(t)$ .

When the stress field is isotropic, as in our studied system, both  $P_{xx}(t)$  and  $P_{yy}(t)$  fluctuate around a constant level of  $pV$  [51], where  $p$  is the pressure and  $V$  is the volume of system. For 2D systems,  $V$  is replaced by the area of the system  $A$ . We average  $P_{xx}(t)$  and  $P_{yy}(t)$  instantaneously, and then we average over time, to obtain our result for  $pV$  (We note that instead of time averages, one can also compute fluctuations of  $P_{xx}(t)$  and  $P_{yy}(t)$ , which are useful for obtaining the longitudinal viscosity [33].).

## 2.3. Units

To compare with experimental situations easily, we use dimensionless quantities. Lengths are normalized by the Debye length  $\lambda_D$ . Energies and temperatures  $k_B T$  are normalized by  $Q^2/4\pi\epsilon_0\lambda_D$ , i.e. the potential energy between two particles separated by a distance of the Debye length. We will write the normalized temperature as  $\mathbb{T} = k_B T / (Q^2/4\pi\epsilon_0\lambda_D)$ .

We normalize pressure  $p$ , which has units of energy per area in 2D systems, two ways. Usually, we normalize pressure as  $\mathbb{P} = p / [(Q^2/4\pi\epsilon_0\lambda_D) / (\pi\lambda_D^2)] = (p4\pi^2\epsilon_0\lambda_D^3) / Q^2$ . This normalization is independent of the kinetic temperature. In choosing this as the normalization, we essentially choose as an energy the unshielded Coulomb potential energy of two particles separated by a distance  $\lambda_D$ , and then we divide it by the area of  $\pi\lambda_D^2$ , to obtain an energy per unit area. Alternatively, for when we have only a single value of  $\kappa$ , we can normalize pressure using a distance  $a$  instead of  $\lambda_D$ , as in

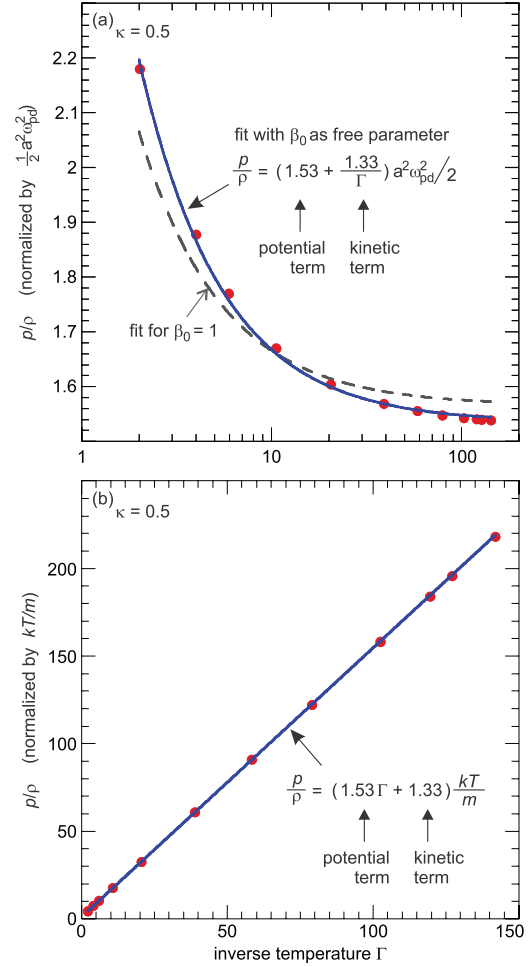


**Figure 1.** Pressure of 2D Yukawa liquids for  $\kappa = 0.5$ . The same simulation data are plotted as circle symbols in the unit of constant  $a^2\omega_{pd}^2/2$  in (a) or in the unit of  $k_B T/m$  (related to  $\Gamma$  values) in (b). The curves shown are fits to equation (2). These fits are done two ways in (a): the solid curve allows the kinetic term multiplier  $\beta_0$  to be a free parameter, yielding a good fit, while the dashed curve assumes  $\beta_0$  to be unity which yields a worse fit. In (b) we show the linear scaling result from (a) again with different scales, to reveal the linear scaling.

figure 1 in section 4.1, where the pressure is normalized by  $(Q^2/4\pi\epsilon_0a)/(1/n) = \rho a^2 \omega_{pd}^2/2$ .

## 3. Expression for pressure

We seek an analytic approximate expression for the pressure. Motivated by the form of equation (1) for stress, we choose a straightforward sum of a potential term and a kinetic term. The potential term is chosen as a simple multiple of the potential energy,  $U_0 = Q^2/(4\pi\epsilon_0a)$ , which is the Coulomb potential energy at a distance of the Wigner–Seitz radius  $a$ . The multiplier  $\alpha_0$  is allowed to be a fit parameter. The resulting analytic expression for the potential term is much less complicated than equation (4.9) of [46]. The kinetic term is chosen as a multiple  $\beta_0$  of the one for an ideal gas; unlike [30, 46, 48] we will investigate whether a better fit can be obtained by allowing the multiplier  $\beta_0$  to differ from unity; we will later remark upon a possible physical justification for a nonzero  $\beta_0$ .

Thus, our conjecture is that the equation of pressure can be written as  $p/\rho = \beta_0 k_B T/m + \alpha_0 U_0/m$ , which we can rewrite as

$$p/\rho = (\alpha_0 + \beta_0/\Gamma) a^2 \omega_{pd}^2/2. \quad (2)$$

We expect that the dimensionless coefficients  $\alpha_0$  and  $\beta_0$  will depend on the physics of screening, and therefore will depend on density or  $\kappa$ .

In section 4.1 we will begin by testing equation (2) by computing the pressure for a single value of  $\kappa = 0.5$ . This result will also help in discussing the physical nature of the terms in the expression of pressure. We will also find values for the dimensionless coefficients  $\alpha_0$  and  $\beta_0$ . Then, in section 4.2 we will prepare a more general equation of pressure by varying  $\kappa$  in our simulation; fitting those results yields a useful analytic expression for a more general expression of pressure.

## 4. Results

### 4.1. Pressure for $\kappa = 0.5$

For a single value of  $\kappa = 0.5$ , figure 1 shows our results for the 2D Yukawa liquid pressure. Two panels are shown, for the two normalizations of pressure, one is  $\rho a^2 \omega_{pd}^2/2$  mentioned above and the other is  $\rho k_B T/m$  related to  $\Gamma$  values. The trend of the data points in figure 1(a) is that the pressure decreases monotonically as the coupling parameter  $\Gamma$  increases. In other words, the pressure decreases when the temperature drops, as expected.

We test equation (2) by fitting to simulation data two ways: with the kinetic term coefficient  $\beta_0$  as a free parameter, and with  $\beta_0$  set to unity. These two fits are shown as solid and dashed curves, respectively, in figure 1(a). We find that equation (2) fits the obtained pressure well when  $\beta_0$  is a free parameter: for  $\kappa = 0.5$  case shown here the best results are for  $\alpha_0 = 1.53$  and  $\beta_0 = 1.33$ . The scaling has a simpler appearance of a straight line if we plot the data differently. This is done using the alternate normalization for  $p$ ,  $k_B T \rho/m$ , in figure 1(b).

We now discuss the physical nature of the potential and kinetic terms in the equation of pressure. If we turn off the potential energy contributions by setting  $\alpha_0$  to zero, so that the only contribution is the kinetic term, then equation (2) would be  $p \propto \beta_0 T$ , which resembles the ideal gas law. This is reasonable because the ideal gas law only contains kinetic effects.

The potential term arises from the microscopic interactions of all the particles. We must recognize that its magnitude, as expressed by the coefficient  $\alpha_0$ , will depend on the microscopic structure and the interactions for a specific system.

The potential term generally dominates the kinetic term for the pressure in a liquid. This is seen in figure 1 over the entire range of the temperatures (or  $\Gamma$ ), for  $\kappa = 0.5$ . The ratio of the potential and kinetic terms is of order  $\Gamma$ , based on a simple comparison of the two terms in the fit result,  $1.53$  for the potential term plus  $1.33/\Gamma$  for the kinetic term. Recall that  $\Gamma > 1$  for a liquid (In the next section we will broaden our study to include a range of  $\kappa$ , which is equivalent to a range of system volumes or areas.).

Having confirmed that our conjecture for the expression of the pressure, equation (2), is reasonable for one value of  $\kappa$ , i.e. one value of area, we next turn to a broader study of the equation of pressure by allowing  $\kappa$  or area to vary.

### 4.2. Pressure for a wide range of $\kappa$

We now study the pressure of the 2D Yukawa liquid over a wide range of parameters. In our MD simulations, we vary temperature  $k_B T$  and density  $\kappa$ , while keeping the simulated system size unchanged. However, in our data analysis, we assume that the Debye length  $\lambda_D$  is constant for various  $\kappa$  values so that we can compare different runs easily. That is to say, our analysis method is equivalent to changing the Wigner–Seitz radius  $a$  or areal number density  $n$  by varying  $\kappa \equiv a/\lambda_D$  [35] while holding the Debye length  $\lambda_D$  constant. Thus, an isochore in our data will correspond to a curve of constant  $\kappa$ .

We will use our conjecture for the expression of pressure, equation (2), in the dimensionless form

$$p = [\alpha + \beta(k_B T 4\pi\epsilon_0\lambda_D/Q^2)] \frac{Q^2}{(4\pi^2\epsilon_0\lambda_D^3)}, \quad (3)$$

or

$$\mathbb{P} = \alpha + \beta\mathbb{T}. \quad (4)$$

Here,  $\mathbb{P} = p(4\pi^2\epsilon_0\lambda_D^3/Q^2)$  is the normalized dimensionless pressure, and  $\mathbb{T} = T(k_B 4\pi\epsilon_0\lambda_D/Q^2)$  is the normalized dimensionless temperature. Note that, since normalizations in equation (4) are different from those in equation (2), the fitting coefficients are different:

$$\kappa^3\alpha = \alpha_0, \quad (5)$$

$$\kappa^2\beta = \beta_0. \quad (6)$$

Our results for the pressure from the simulation are presented as data points in figure 2. The data are organized according to the value of  $\kappa$ , i.e. according to isochores. The range of  $\kappa$  shown is  $0.5$ – $3.0$ , which covers all typical dusty plasma experiments [13, 52]. As expected, the pressure of a 2D Yukawa liquid increases with temperature for all simulated conditions.

We also indicate the phase transition in the pressure–temperature space, in figure 2. The dashed curve is the phase-transition, based on the data from other MD simulations [30, 36] which were reported in the  $\Gamma - \kappa$  space; we convert those previously published  $\Gamma - \kappa$  melting curves to the pressure–temperature space by using our pressure data in figure 2.

As the main result of the paper, we find that the analytic approximation of the equation of pressure, equation (4), shows excellent agreement with the simulation, over a wide range of temperatures and densities. The discrepancy is generally very small, as seen by comparing the data points for the simulation and the smooth curves for the analytic approximation in figure 2. The largest percentage discrepancy, as indicated by a gap between data points and curve on the log–log plot, is found in the lower left corner, for low temperature and large  $\kappa$  values, i.e. cold low density liquids.



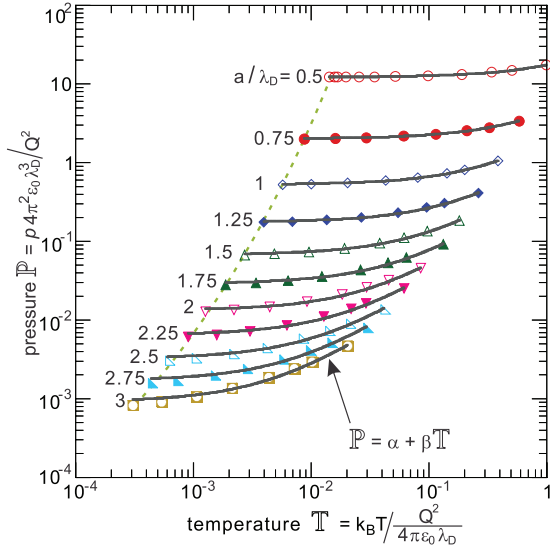


**Figure 2.** Pressure of 2D Yukawa liquids for various values of  $\kappa = a/\lambda_D$  where  $a$  is the Wigner–Seitz radius. Curves fit the expression of  $\mathbb{P} = \alpha + \beta\mathbb{T}$  quite well. A curve corresponds to an isochore. The solid–liquid phase transition of the 2D Yukawa system is shown as a dashed line. We obtain the pressure data from our simulation, using the melting points of 2D Yukawa liquids (expressed in terms of  $\Gamma$  for different  $\kappa$ ) from previous simulations [30, 36]. Solids are to the left of the dashed curve, while liquids (which are studied in this paper) are to the right.

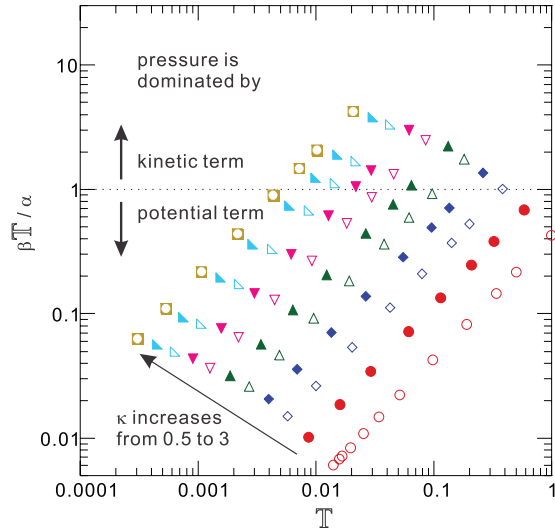


**Figure 3.** The ratio of the kinetic contribution and the potential contribution to the pressure for different temperatures and densities. Symbols are plotted in the same style as in figure 2, for different  $\kappa$  values. A dotted line for a ratio of unity indicates where the two contributions are equal.

The physics interpretation of equation (4) is that the pressure of 2D Yukawa liquids is composed of two contributions. The potential term with the coefficient  $\alpha$  is independent of temperature; it depends on density or  $\kappa$  because it is determined by the potential energy for particles arranged spatially with the microstructure of a liquid. The kinetic term with the coefficient  $\beta\mathbb{T}$  increases linearly with temperature, much like the ideal gas law.

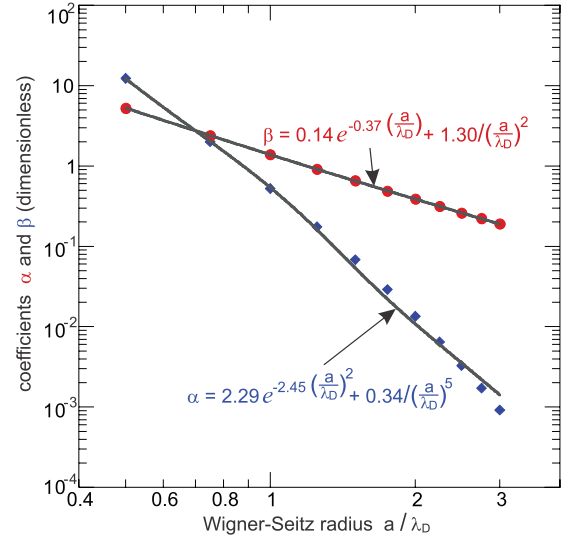


**Figure 4.** The coefficients  $\alpha$  and  $\beta$ . The data points are from the fits in figure 2, while the curves are fits to equations (5) and (6).

To compare the contributions from the potential and kinetic parts of the pressure, we plot the ratio of these two parts in figure 3. Generally, the kinetic term dominates at the top of the graph, for large values of  $\mathbb{T}$ , while the potential term dominates at the bottom. The dividing line, where the potential and kinetic terms are equal, is  $\mathbb{T} = \alpha(\kappa)/\beta(\kappa)$ , shown as a dotted line.

We present the coefficients  $\alpha$  and  $\beta$  and their dependence on  $\kappa$  in figure 4. We find the values of these coefficients by allowing them to be the two free parameters in the fit to equation (4). We see that both  $\alpha$  for the potential term and  $\beta$  for the kinetic term decrease with  $\kappa$ , i.e. they decrease with area of one particle, or the averaged particle spacing. In other words, both contributions to the pressure depend on density in the same way, although the potential term has a much stronger dependence as indicated by the greater slope in figure 4.

As an analytic approximation, we find that these coefficients can be fit to the following expressions

$$\alpha = 2.29e^{-2.45(a/\lambda_D)^2} + 0.34/(a/\lambda_D)^5 \quad (7)$$

$$\beta = 0.14e^{-0.37(a/\lambda_D)} + 1.30/(a/\lambda_D)^2. \quad (8)$$

These expressions are plotted in figure 4 as smooth curves. The discrepancy compared to the data points for the simulation is small, for the experimentally relevant range of parameters that we studied here. The data plotted in figure 4 for  $\alpha$  and  $\beta$  can be converted to  $\alpha_0$  and  $\beta_0$  using equations ((5)–(6)). Over the range of  $a/\lambda_D$  shown in figure 4, the variation of  $\beta$  corresponds to  $\beta_0$  increasing from 1.325 to 1.724.

It deserves mention that our coefficient  $\beta_0$  has a value that differs from unity. This phenomenological result might be unexpected. The kinetic term in equation (1) has no adjustable multiplier, so that one might just assume that such a multiplier must have a value of unity, and this is indeed commonly assumed when using other methods as well [30, 46–49]. If we did not allow  $\beta_0$  to differ from unity, our fit would be poor as shown by the dashed curve in figure 1(a). We should ask

what is the significance, then, of our phenomenological result that  $\beta_0 > 1$ . One possibility is that it essentially captures the temperature dependence of the potential term, which arises from the temperature variation in microscopic structure (as measured for example by pair correlation functions).

## 5. Conclusion

Using an MD simulation, we have obtained an analytic approximation for the pressure of a 2D Yukawa liquid, valid over a wide range of parameters. We did this by computing the pressure, and modeling it as the sum of two terms, potential and kinetic, where the kinetic term is proportional to temperature and the potential term is independent of temperature.

The resulting equation of pressure is equation (4) with equations ((7) and (8)). In these equations, the parameters  $\alpha$  for the potential term and  $\beta$  for the kinetic term are functions only of area, or  $\kappa$  when the Debye length  $\lambda_D$  is held constant.

## Acknowledgments

Work in China was supported by the National Natural Science Foundation of China under Grant No. 11505124, the 1000 Youth Talents Plan, and the startup funds from Soochow University. Work at the University of Iowa was supported by NSF and the Department of Energy.

## References

- [1] Perrot P 1998 *A to Z of Thermodynamics* (Oxford: Oxford University Press)
- [2] Fetter A L and Walecka J D 2003 *Theoretical Mechanics of Particles and Continua* (Mineola: Dover)
- [3] van der Waals J D 1873 On the continuity of the gaseous and liquid states *Doctoral Dissertation* Leiden University, Leiden, The Netherlands
- [4] MacDonald J R 1969 *Rev. Mod. Phys.* **41** 316
- [5] Yamada M, Stanley H E and Sciortino F 2003 *Phys. Rev. E* **67** 010202
- [6] Gandolfi S, Illarionov A Y, Schmidt K E, Pederiva F and Fantoni S 2009 *Phys. Rev. C* **79** 054005
- [7] Yukawa H 1935 *Proc. Phys. Math. Soc. Japan* **17** 48
- [8] Konopka U, Morfill G E and Ratke L 2000 *Phys. Rev. Lett.* **84** 891
- [9] Safran S A 2003 *Statistical Thermodynamics of Surfaces, Interfaces, and Membranes* (Boulder, CO: Westview)
- [10] Feng Y, Goree J, Liu B and Cohen E G D 2011 *Phys. Rev. E* **84** 046412
- [11] Shukla P K and Mamun A A 2002 *Introduction to Dusty Plasma Physics* (Bristol: IOP)
- [12] Fortov V E, Ivlev A V, Khrapak S A, Khrapak A G and Morfill G E 2005 *Phys. Rep.* **421** 1
- [13] Morfill G E and Ivlev A V 2009 *Rev. Mod. Phys.* **81** 1353
- [14] Piel A 2010 *Plasma Physics* (Heidelberg: Springer)
- [15] Bonitz M, Henning C and Block D 2010 *Rep. Prog. Phys.* **73** 066501
- [16] Melzer A, Homann A and Piel A 1996 *Phys. Rev. E* **53** 2757
- [17] Nosenko V and Goree J 2004 *Phys. Rev. Lett.* **93** 155004
- [18] Chan C-L, Woon W-Y and Lin I 2004 *Phys. Rev. Lett.* **93** 220602
- [19] Nunomura S, Zhdanov S, Samsonov D and Morfill G 2005 *Phys. Rev. Lett.* **94** 045001
- [20] Knapek C A, Samsonov D, Zhdanov S, Konopka U and Morfill G E 2007 *Phys. Rev. Lett.* **98** 015004
- [21] Sheridan T E 2008 *Phys. Plasmas* **15** 103702
- [22] Io C-W and Lin I 2009 *Phys. Rev. E* **80** 036401
- [23] Hartmann P, Kovács A Z, Douglass A M, Reyes J C, Matthews L S and Hyde T W 2014 *Phys. Rev. Lett.* **113** 025002
- [24] Shahzad A and He M G 2012 *Contrib. Plasma Phys.* **52** 667
- [25] Shahzad A and He M G 2012 *Contrib. Phys. Plasmas* **19** 083707
- [26] Shahzad A and He M G 2012 *Plasma Sci. Technol.* **14** 771
- [27] Shahzad A and He M G 2013 *AIP Conf. Proc.* **1547** 173
- [28] Ludwig P, Miloch W J, Kählert H and Bonitz M 2015 *New J. Phys.* **14** 053016
- [29] Donkó Z, Hartmann P and Kalman G J 2004 *Phys. Rev. E* **69** 065401
- [30] Hartmann P, Kalman G J, Donkó Z and Kutasi K 2005 *Phys. Rev. E* **72** 026409
- [31] Hartmann P, Kalman G J and Donkó Z 2006 *J. Phys. A: Math. Gen.* **39** 4485
- [32] Hartmann P, Donkó Z, Bakshi P M, Kalman G J and Kyrkos S 2007 *IEEE Trans. Plasma Sci.* **35** 332
- [33] Feng Y, Goree J and Liu B 2013 *Phys. Rev. E* **87** 013106
- [34] Feng Y, Goree J, Liu B, Intrator T P and Murillo M S 2014 *Phys. Rev. E* **90** 013105
- [35] Kalman G J, Hartmann P, Donkó Z and Rosenberg M 2004 *Phys. Rev. Lett.* **92** 065001
- [36] Ott T, Stanley M and Bonitz M 2011 *Phys. Plasmas* **18** 063701
- [37] Liu B and Goree J 2005 *Phys. Rev. Lett.* **94** 185002
- [38] Donkó Z and Hartmann P 2007 *Modern Phys. Lett. B* **21** 1357
- [39] Shahzad A and He M G 2012 *Phys. Scr.* **86** 015502
- [40] Shahzad A and He M G 2013 *Phys. Scr.* **87** 035501
- [41] Shahzad A and He M G 2015 *Int. J. Thermophys.* **36** 2565
- [42] Shahzad A and He M G 2015 *Phys. Plasmas* **22** 123707
- [43] Melzer A, Nunomura S, Samsonov D, Ma Z W and Goree J 2000 *Phys. Rev. E* **62** 4162
- [44] Nunomura S, Goree J, Hu S, Wang X and Bhattacharjee A 2002 *Phys. Rev. E* **65** 066402
- [45] Nosenko V, Goree J, Ma Z W, Dubin D H E and Piel A 2003 *Phys. Rev. E* **68** 056409
- [46] Totsuji H, Liman M S, Totsuji C and Tsuruta K 2004 *Phys. Rev. E* **70** 016405
- [47] Totsuji H 2006 *J. Phys. A: Math. Gen.* **39** 4493
- [48] Vaulina O S and Koss X G 2009 *Phys. Lett. A* **373** 3330
- [49] Vaulina O S, Khrustalyov Yu V, Petrov O F and Fortov V E 2010 *Europhys. Lett.* **89** 35001
- [50] Oxtoby N P, Griffith E J, Durniak C, Ralph J F and Samsonov D 2013 *Phys. Rev. Lett.* **111** 015002
- [51] Hoheisel C 1987 *J. Chem. Phys.* **86** 2328
- [52] Feng Y, Goree J and Liu B 2010 *Phys. Rev. Lett.* **105** 025002